

Study of heat capacity enhancement in some nanostructured materials*

Zhi-Cheng Tan[‡], Lan Wang, and Quan Shi

Thermochemistry Laboratory and China Ionic Liquids Laboratory, Dalian Institute of Chemical Physics, Chinese Academy of Sciences, Dalian 116023, China

Abstract: Heat capacity properties of some nanostructured oxides, metals, and zeolites were studied, mainly with the aid of low-temperature adiabatic calorimetry. Obvious enhancement in the heat capacity of nanostructured materials to different degrees was observed as compared with the corresponding coarse-grained materials. The contributions of enhanced heat capacity of nanostructured materials toward properties such as density, thermal expansion, sample purity, surface effect, and size effect are discussed.

Keywords: adiabatic calorimetry; heat capacity enhancement; nanostructured metals; nanostructured oxides; nanostructured zeolite.

INTRODUCTION

In recent years, nanostructured materials have gained worldwide attention owing to their special properties. Due to their small grain size and large specific surface, nanostructured materials exhibit many distinctive properties [1]. These properties, in turn, raise distinctive questions. What are the special thermodynamic properties of nanostructured materials constructed from nanosized particles? Can classical thermodynamic theories be used to explain the thermal behavior of nanostructured materials? Those are some of the important questions that must be answered in order to understand the properties of nanostructured materials more thoroughly and broaden their areas of application.

Experimental measurements of heat capacity at constant pressure indicate that heat capacity values of nanostructured materials are frequently higher than those of coarse-grained materials [2–8]. For example, the heat capacity enhancement in going from the polycrystalline to the nanocrystalline state varies between 29 and 53 % for particle size of 6 nm palladium over the temperature range from 150 to 300 K. Computer simulation results on theoretical calculations showed that heat capacity of grain boundary increase with an increment of the grain boundary excess volume [9,10]. Wolf et al. [11] reported thermodynamic properties of nanocrystalline materials and glasses, implying that the excess specific heat depends on grain size. Recently, research work on rutile and anatase nanoparticles carried out by Boerio-Goates et al. [12] concluded that the high energies associated with nanoparticle surfaces must be stabilized by adsorption of water or other solvents onto the nanoparticle surfaces, and that neglect of the presence of these contaminants or capping agents can lead to the appearance of positive excess specific heat that is not present when the specific heat of the surface is taken into account. However, analyses of the heat capacity enhancements in the nanostructured materials relative to the coarse-grained materials are much more complicated.

*Paper based on a presentation at the 20th International Conference on Chemical Thermodynamics (ICCT 20), 3–8 August 2008, Warsaw, Poland. Other presentations are published in this issue, pp. 1719–1959.

[‡]Corresponding author

Adiabatic calorimetry is a classical technique that is usually used in the fields of thermochemistry. It is the most accurate method for the measurement of heat capacities of materials. Heat capacity is one of the fundamental thermodynamic data of materials and is very important to many physical and chemical theoretical researches and engineering technology design concerned with materials. Many other thermodynamic properties, such as enthalpy, entropy, and Gibbs free energy can be calculated from highly precise heat capacity data [13]. Hence, much work has been done to measure heat capacities with adiabatic calorimetric instruments throughout the world [14–26].

In this work, we have measured heat capacity of various kinds of nanostructured oxides, metals, and zeolites, mainly with the aid of low-temperature adiabatic calorimetry [24–26], and compare heat capacity enhancement in these materials with the corresponding coarse-grained materials. These data are discussed in the context of properties such as density, thermal expansion, sample purity, surface effect, and size effect. Synthesis of nanostructured materials has been accompanied by adiabatic calorimetry measurements, and materials have been characterized with the aid of differential scanning calorimetry (DSC), thermogravimetric (TG) analysis, thermal expansion coefficient measurements, X-ray diffraction (XRD), transition electron microscopy (TEM), scanning electron microscopy (SEM), X-ray fluorescence (XRF), and infrared spectroscopy (IR). Full details about the synthesis and characterization of materials are published elsewhere [27].

ADIABATIC CALORIMETRY

The heat capacity measurements were made by an adiabatic calorimetric system for small samples over the temperature range from 78 to 400 K. The construction of the calorimeter has been described previously [24] in detail. It mainly consisted of a sample cell, two (inner and outer) adiabatic shields, two sets of differential thermocouples, a vacuum can, and a Dewar vessel. The sample cell was 6 cm³ in inner volume, made of gold-plated copper and equipped with a miniature platinum resistance thermometer and a heater. The sample cell was in turn surrounded by the inner and outer adiabatic shields. A small amount of helium gas was introduced into the cell to enhance the heat transfer inside the whole cell. Liquid nitrogen was used as the cooling medium. The evacuated can was immersed in liquid nitrogen and kept within 10^{−3} Pa vacuum to eliminate the heat loss owing to the gas convection. The two adiabatic shields were made of chromium-plated copper and equipped with manganin heating wires. The two sets of six-junction chromel-contantan (Ni 55 %, Cu 45 %) thermocouples were mounted on the cell and the two shields to measure the temperature differences between the sample cell and the inner adiabatic shield and between the inner and the outer adiabatic shields, respectively. The temperatures of the two shields were controlled separately and automatically with two units of auto-adiabatic controller. The miniature platinum resistance thermometer (IPRT No. 2, 16 mm in length, 1.6 mm in diameter, a nominal resistance of $R_0 = 100 \Omega$, produced by Shanghai Institute of Industrial Automatic Meters, calibrated on the basis of ITS-90, calibrated by the Center of Low-Temperature Metrology and Measurement, Academia Sinica) was applied to measure the temperature of the sample. The sample was heated using the standard discrete heating method, and the temperature of the sample was alternatively measured by use of a precision digital multimeter. The heating duration was about 600 s, the equilibrium time of each temperature point is about 300 s, and the temperature drift rates of the sample cell in an equilibrium period were usually within 10^{−3}–10^{−4} K min^{−1}. During the heat capacity measurements, the temperature difference between the inner adiabatic shield and the sample cell was automatically kept within 10^{−3} K min^{−1} in order to obtain a satisfactory adiabatic effect and the corresponding equilibrium temperature was corrected for heat loss.

Before the heat capacity measurement of the sample, the reliability of the calorimetric apparatus was verified by heat capacity measurements of the standard reference material α -Al₂O₃ (NIST SRM-720). Deviations of the experimental results from the smoothed curve lie within ± 0.2 %, while the inaccuracy is within ± 0.5 %, as compared with the recommended value reported by D. G. Archer [21] over the whole experimental temperature range.

NANOSTRUCTURED OXIDES

Nanostructured oxide materials constitute a rich source of materials. We selected five kinds of oxide materials, Al_2O_3 , SiO_2 , TiO_2 , ZnO_2 , and ZrO_2 , which have been widely used, can be prepared by classical methods and obtained with confined size range and high quality.

Nanostructured Al_2O_3

We studied molar heat capacity of nanostructured Al_2O_3 in the temperature range from 78 to 370 K, and compared with the coarse-grained Al_2O_3 [28]. The nanopowder Al_2O_3 was processed by the technique of hydrolysis of pure aluminum sheet after activation, and the sample purity is more than 99 %. The coarse-grained sample of $\alpha\text{-Al}_2\text{O}_3$ is a commercial reagent purchased from Shanghai Chemical Reagent Factory with the purity of 99.9 %. Figure 1 shows the experimental results indicating that no thermal anomaly took place over the investigated temperature range, but the heat capacities of the nanostructured Al_2O_3 were larger than the coarse-grained one and increased with the size decreased. The nanostructured Al_2O_3 has excess heat capacity from 6 to 23 % as compared with the coarse-grained one in the temperature range from 200 to 370 K. In the study of infrared spectra, we found that nanostructured Al_2O_3 exhibited a blue shift in wave number. This shift indicates that energy structure of nanostructured Al_2O_3 is higher than that in a coarse-grained state, which is in agreement with the results of heat capacity measurement. To further study the enhancement of heat capacity in nanostructured Al_2O_3 , we measured the density of nanostructured Al_2O_3 to be 89 % of the coarse-grained one, and thermal expansion of nanostructured Al_2O_3 has been reported to be twice as that of the conventional [29]. All these suggest that the grain boundary of nanostructured materials possesses an excess volume with respect to the perfect crystal lattice, so it seems that the heat capacity enhancement in nanostructured Al_2O_3 results from the excess volume.

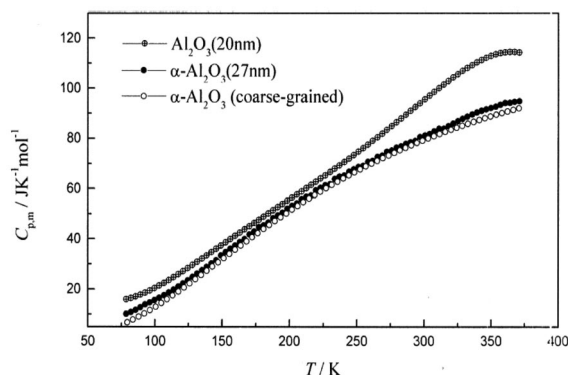


Fig. 1 Heat capacity of nanostructured and coarse-grained Al_2O_3 .

Nanostructured amorphous SiO_2

The molar heat capacity of nanostructured amorphous SiO_2 (na- SiO_2) was measured over the temperature range from 9 to 354 K. The samples used for experiment were synthesized by using the sol-gel route with hydrolyzing the ethyl tetrasilicate and controlling the chemical reaction conditions. Those samples possess a very high purity (>99.9 %). The experimental results were plotted in Fig. 2 together with the molar heat capacity of coarse-grained SiO_2 (ca- SiO_2) [30]. The average grain size of two amorphous SiO_2 is also 20 nm, and their specific surfaces resulted from Brunauer–Emmett–Teller (BET) measurement are $160 \text{ m}^2/\text{g}$ ($\text{SiO}_2\text{-1}$) and $640 \text{ m}^2/\text{g}$ ($\text{SiO}_2\text{-2}$), respectively. Significant difference

in heat capacity between na-SiO₂ and ca-SiO₂ can be identified from Fig. 2. The heat capacity enhancement from 150 to 350 K for na-SiO₂-1 and na-SiO₂-2 are about 2–7 % and 4–10 % higher than those of ca-SiO₂, respectively. The heat capacity values of SiO₂-2 with larger specific surface are higher about 3 % than those of SiO₂-1. The heat capacity enhancements in the nanostructured materials are usually associated with an increase in the configuration and vibrational entropy of grain boundaries, and the boundaries with larger specific surface will have more configuration and vibrational entropy. So it agrees well with the experimental results that larger grain surface has much contribution to the heat capacity enhancement. We calculated the thermodynamic functions of na-SiO₂ based on the heat capacity data. The calculated results were plotted in Fig. 3. From Fig. 3, we can obtain that the entropy, enthalpy, and Gibbs free energy of larger specific surface na-SiO₂ is higher than those of the small one, and the Gibbs free energy is lower, implying larger specific surface materials have complicated disorder, large potential energy, and high activity.

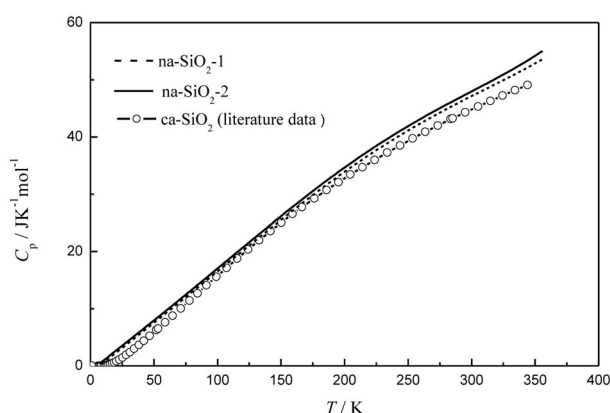


Fig. 2 Heat capacity of nanostructured amorphous and coarse-grained SiO₂ as functions of temperature.

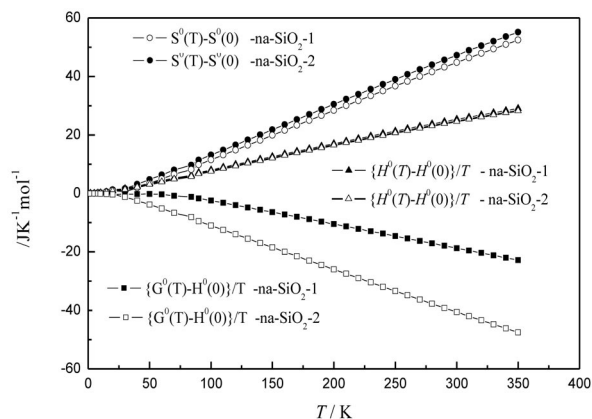


Fig. 3 Entropy, enthalpy, and Gibbs free energy of nanostructured amorphous SiO₂ as functions of temperature.

Nanocrystalline ZnO

The two nanocrystalline forms of ZnO studied are ZnO-1 and ZnO-2 with grain size of 65 and 18 nm, respectively. The purity of both two samples is more than 99 %. Heat capacity of nanocrystalline ZnO was compared with the literature data [31] of coarse-grained ZnO (c-ZnO) in Fig. 4. It can be seen that

the heat capacities of ZnO-1 are not obviously different from that of c-ZnO. However, there is large excess heat capacity of 4–17 % for ZnO-2 compared with c-ZnO. The similar result was also reported by other researchers [2,3]. Heat capacity of a material is directly related to its atomic structure or its vibrational and configurational entropy, which is significantly affected by the nearest-neighbor configurations. Nanocrystals are structurally characterized by the ultrafine crystalline grains, and a large fraction of atoms located in the metastable grain boundaries in which the nearest-neighbor configurations are much different from those in the crystallites. In other words, the grain boundary possesses an excess volume with respect to the perfect crystal lattice. Therefore, heat capacities of nanocrystals are higher than those of the corresponding coarse-grained polycrystalline counterparts. Although slight impurity can enhance the heat capacity obviously [32], the impurity effect on those two specimens should be very slight. The samples were heated at the temperature of 570 K for 2 h, and sample cells were evacuated to be high vacuum (10^{-5} Pa), which can remove the absorbed gas and vapor. So the main contribution of the excess heat capacity in nanocrystalline ZnO-2 should be introduced by vibrational and configurational entropy due to grain boundaries and lattice defects.

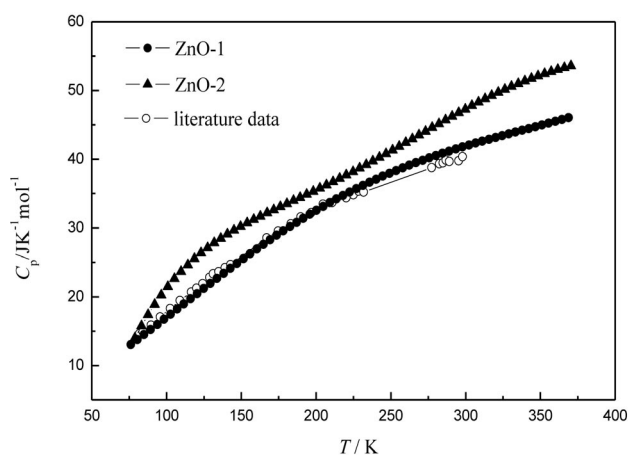


Fig. 4 Heat capacity of nanocrystalline ZnO and the literature heat capacity data of coarse-grained crystalline ZnO.

It seems to contradict our understanding of the above excess heat capacity, that nanocrystalline ZnO-1 and the more coarse-grained ZnO display very little difference. In fact, the grain size effect of nanocrystals on heat capacity has a size limit [32]. If the grain size is lower than the limit, the heat capacity will exhibit a great increase. Otherwise, the heat capacity of nanocrystals and conventional polycrystals has little difference.

Nanocrystalline TiO₂

We measured the heat capacity of nanocrystalline TiO₂ with three grain sizes by adiabatic calorimetry. TiO₂-2 and TiO₂-3 are anatase phase with the purity of 99 %, and TiO₂-1 is mainly anatase with a small amount of brookite phase. The experimental results were compared with reported heat capacity of coarse-grained anatase phase TiO₂ [33] in Fig. 5. It is very obvious that the heat capacity of nanocrystalline was enhanced, and the heat capacities increase with grain size decreasing. The heat capacity enhancement of TiO₂-1 and TiO₂-2 was plotted in Fig. 6. In the temperature range from 100 to 300 K, the heat capacity enhancements of TiO₂-1 and TiO₂-2 were 7–13 and 4–7 %, respectively. The heat capacity enhancement of TiO₂-1 relative to TiO₂-2 was 3–6 %, while the enhancement of TiO₂-2 relative to TiO₂-3 was only about 1 %. Considering the size-decreasing step is equal from

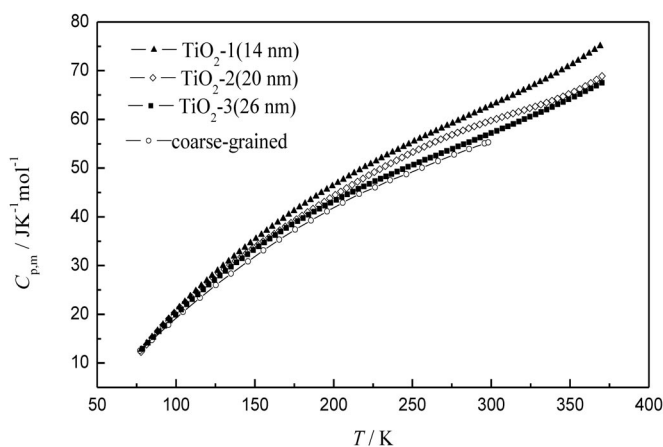


Fig. 5 Heat capacity of anatase phase nanocrystalline TiO_2 with different grain sizes.

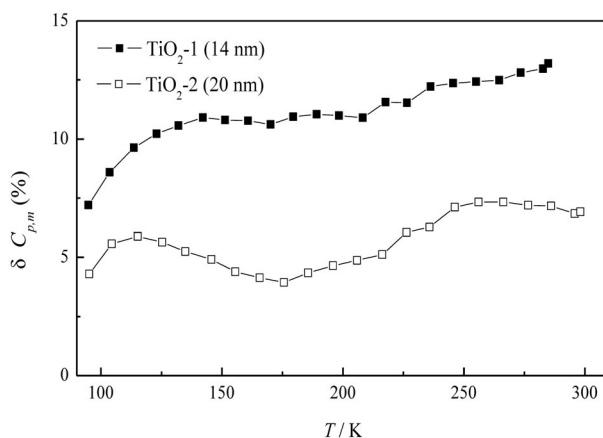


Fig. 6 Heat capacity enhancement of nanocrystalline TiO_2 as a function of temperature, $\delta C_{p,m} (\%) = 100 \% * [C_{p,m}(\text{nano}) - C_{p,m}(\text{coarse})] / C_{p,m}(\text{coarse})$.

TiO_2 -3 to TiO_2 -2 and from TiO_2 -2 to TiO_2 -1, the nanocrystalline size is not the main factor affecting the heat capacity enhancement in this case. The sample of TiO_2 -1 contains mainly anatase phase with a small amount of brookite phase and the samples of TiO_2 -2 and TiO_2 -3 are all anatase phase, so we can draw a conclusion that the small amount of heteromorphic impurity makes more contribution to the heat capacity enhancement than the grain size. Recently, research work by Boerio-Goats et al. reported that the water or other solvents absorbed on nanoparticle surfaces lead to heat capacity enhancement of anatase phase nanoparticles [12].

Nanocrystalline ZrO_2

Nanocrystalline ZrO_2 with grain size of 18 nm was measured by adiabatic heat capacity calorimetry and compared with literature data of coarse-grained ZrO_2 [34]. The sample was prepared with the method of azeotropic distillation, and the purity is more than 99 %. The heat capacity enhancement of nanocrystalline ZrO_2 was much larger than those of the above nanostructured oxides. The enhancement was about 2–21 % in the temperature range from 100 to 300 K and exhibited a rising tendency with the

temperature increasing. Many researchers theoretically explained the excess heat capacity of nanostructured materials by excess volume, and some theoretical calculations have indicated that heat capacity enhancement sharply increases with the excess volume increasing when temperature rises [10]. We measured the density of the nanocrystalline ZrO_2 sample (5.2 g cm^{-3}) to be 93 % of the coarse-grained ZrO_2 (5.6 g cm^{-3}). This difference in density is not very obvious and can hardly lead to 2–21 % of heat capacity enhancement. We also measured the chemical purity of the nanocrystalline ZrO_2 to be 98.4 %, so the contribution of impurity contained in the nanocrystalline to heat capacity enhancement cannot be neglected. We presume that heat capacity enhancement in the nanocrystalline ZrO_2 is mainly caused by impurity contained in it. Impurity in nanostructured materials is not the general case of adulteration, since it is not avoided in the process of sample preparation, but it can bring activity to the materials. So nanocrystalline ZrO_2 has higher activity than the coarse-grained one and is mostly used as a catalyst in some reactions.

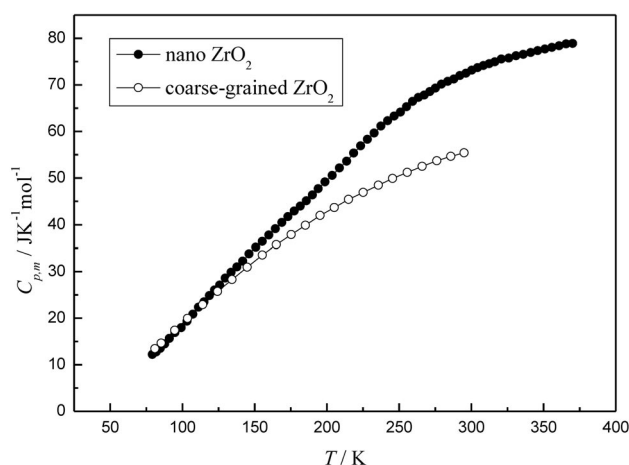


Fig. 7 Heat capacity of nanocrystalline ZrO_2 and the literature heat capacity data of coarse-grained crystalline ZrO_2 .

NANOCRYSTALLINE METALS

Nanocrystalline metals are studied mostly in theory because their molecular structure is simple and easily calculated and explained. Those materials differ from glasses and crystals in the sense that they exhibit little short- or long-range order. A series of novel physical and chemical properties of the nanocrystals, such as high diffusivity and reactivity, great ductibility, large thermal expansion, enhanced phonon specific heat, and a significant change in the magnetic susceptibility, relative to the corresponding coarse-grained polycrystals, have captured the attention of the scientists and engineers because of their potential application [1]. We measured heat capacities of nanocrystalline nickel [35] and copper in the temperature range from 78 to 370 K, and studied the heat capacity enhancement relative to the corresponding coarse-grained metal crystal. The two samples were produced by Zhengyuan Nano-materials Engineering Corp. (Shandong, China). The labeled chemical purity is not less than 99 %.

Nanocrystalline nickel

Heat capacity of 40 nm nanocrystalline nickel was plotted in Fig. 8 and compared with the literature data [36] of coarse-grained crystalline nickel. From the insert in the figure we can see that heat capacity

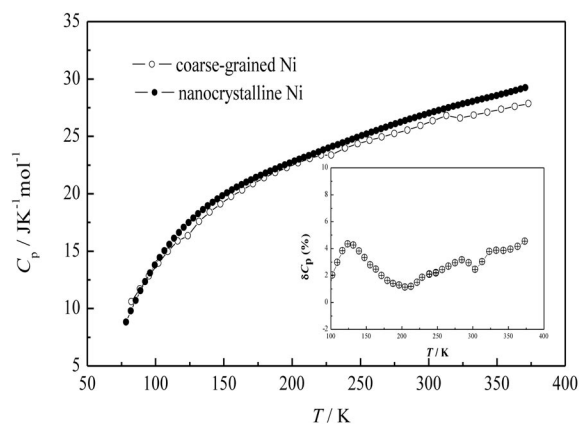


Fig. 8 Heat capacity of nanocrystalline nickel and the literature heat capacity data of coarse-grained crystalline nickel, insert is heat capacity enhancement of nanocrystalline nickel.

enhancement varies between 2 and 4 % in the temperature range from 100 to 370 K. The heat capacity enhancements in nanocrystalline materials are usually associated with an increase in the configurational and vibrational entropy of the grain boundaries, which constitute a large volume fraction of the material. The atomic fraction of the grain-boundary component can be approximately estimated to be $3\delta/d$, where d is the average size of crystalline grain and δ is the average thickness of interfaces, which is known to be on the order of three or four atomic layers. For the nanocrystalline nickel with $d = 40$ nm, about 10 % atoms are on the grain boundaries. Thus, the grain-boundary configurations or the grain-boundary energy should be responsible for the heat capacity enhancement.

Nanocrystalline copper

Figure 9 shows the heat capacity of 50-nm nanocrystalline copper and the literature data [37] of the coarse-grained one. The heat capacity enhancement is about 3–6 % in the temperature range from 100 to 370 K. The purity of nanocrystalline copper is more than 99 %, so the contribution of impurity to the enhancement is almost negligible. The relative density of nanocrystalline copper to the coarse-grained is 51 %, indicating a more open atomic structure of the grain-boundary component than coarse-grained

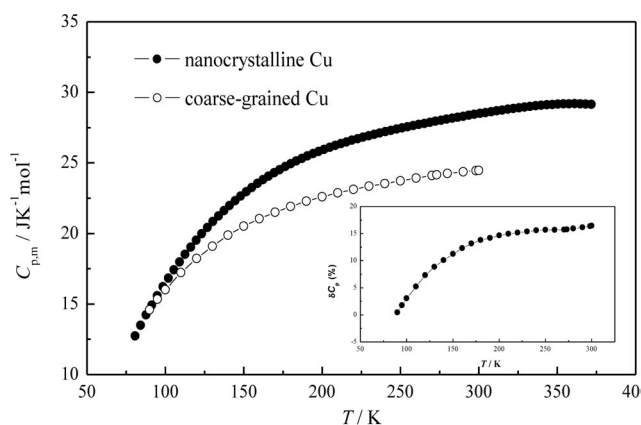


Fig. 9 Heat capacity of nanocrystalline copper and the literature heat capacity data of coarse-grained crystalline copper, insert is heat capacity enhancement of nanocrystalline copper.

polycrystalline copper, so the interatomic coupling becomes weaker and enhances heat capacity. In the theoretical calculation by Fecht et al. [38], the thermal expansion coefficient is related to heat capacity, and the larger the thermal expansion coefficient becomes, the more the heat capacity enhances. We measured thermal expansion coefficient of nanocrystalline copper ($3 \times 10^{-5} \text{ K}^{-1}$) to be about two times of the coarse-grained copper's ($1.6 \times 10^{-5} \text{ K}^{-1}$). Thus, we can also explain the heat capacity enhancement of nanocrystalline copper with the increasing thermal expansion coefficient.

NANO- AND MICROSIZED ZEOLITE

Nanosized zeolite is only different from micro-sized zeolite in the size, but its properties have varied much in some aspects when it changes into micro-sized zeolite. We carried out adiabatic heat capacity measurement on nano- and micro-sized ZMS-5, and compared their thermodynamic properties. From Fig. 10, it can be clearly seen that the heat capacities of nanosized ZMS-5 are larger than the micro-sized one. The heat capacity enhancement in the low temperature is not very obvious, but becomes larger with the temperature increasing. Nanosized ZMS-5 possesses excess specific surface and behaves more actively than the micro-sized. This excess specific surface supplies more surface energy for nanosized ZMS-5 and enhances heat capacity.

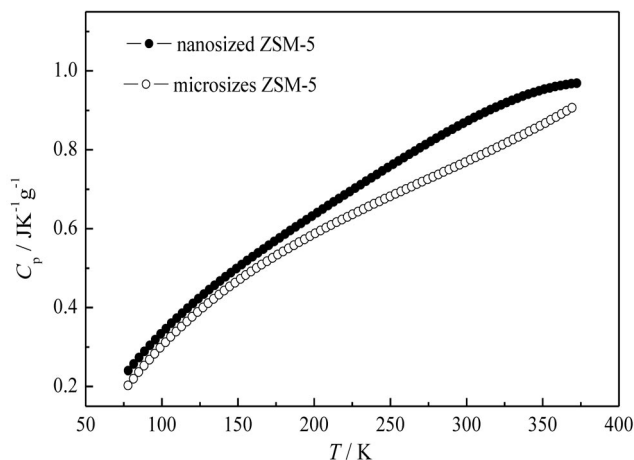


Fig. 10 Heat capacity of nanosized and micro-sized ZSM-5.

CONCLUSION

Heat capacity enhancement in nanostructured materials is influenced by many factors, such as density, thermal expansion, sample purity, surface absorption, size effect, and so on. But the dominant factor affecting heat capacity enhancement is different in different nanostructured materials. Only with careful and entire investigation on the particular properties of nanostructured materials, can we discuss and analyze the heat capacity enhancement. On the other hand, adiabatic calorimetry is the most direct method to measure heat capacity enhancement in nanostructured materials, however, in order to set up thermodynamic theoretical model to describe and understand heat capacity enhancement, more theoretical calculation studies and other experimental measurements should be still and further carried out.

REFERENCES

1. H. Gleiter. *Prog. Mater. Sci.* **33**, 223 (1989).
2. J. Rupp, R. Birringer. *Phys. Rev. B* **36**, 7888 (1987).
3. E. Hellestern, H. J. Fecht, Z. Fu, W. L. Johnson. *J. Appl. Phys.* **65**, 305 (1989).
4. A. Tschöpe, R. Birringer. *Acta Metall. Mater.* **45**, 2719 (1993).
5. Y. Y. Chen, Y. D. Yao, S. S. Hsiao, S. U. Jen, B. T. Lin, H. M. Lin, C. Y. Tung. *Phys. Rev. B* **52**, 9364 (1995).
6. K. Lu, R. Lück, B. Predel. *Z. Metallkd.* **84** (1993).
7. N. X. Sun, K. Lu. *Phys. Rev. B* **54**, 6058 (1996).
8. H. Y. Bai, J. L. Luo, D. Jin, J. R. Sun. *J. Appl. Phys.* **79**, 361 (1996).
9. H. J. Fecht. *Phys. Rev. Lett.* **65**, 610 (1990).
10. M. Wagner. *Phys. Rev. B* **45**, 635 (1992).
11. D. Wolf, J. Wang, S. R. Phillpot, H. Gleiter. *Phys. Lett. A* **205**, 274 (1995).
12. J. Boerio-Goates, G. Li, L. Li, T. F. Walker, T. Parry, B. F. Woodfield. *Nano Lett.* **6**, 750 (2006).
13. Z. C. Tan, Y. Y. Di. *Prog. Chem.* **18**, 1234 (2006).
14. Z. C. Tan, Q. Shi, B. P. Liu, H. T. Zhang. *J. Therm. Anal. Calorim.* **92**, 367 (2008).
15. B. E. Lang, J. Boerio-Goates, B. F. Woodfield. *J. Chem. Thermodyn.* **38**, 1655 (2006).
16. S. L. Randzio. *Annu. Rep. Prog. Chem., Sect. C* **98**, 157 (2002).
17. K. Kobashi, T. Kyomen, M. Oguni. *J. Phys. Chem. Solids* **59**, 667 (1998).
18. M. Sorai, K. Kaji, Y. Kaneko. *J. Chem. Thermodyn.* **24**, 167 (1992).
19. T. Matsuo, H. Suga. *Thermochim. Acta* **88**, 149 (1985).
20. A. Inaba. *J. Chem. Thermodyn.* **15**, 1137 (1983).
21. D. G. Archer. *J. Phys. Chem. Ref. Data* **22**, 1441 (1993).
22. J. T. S. Andrews, P. A. Norton, E. F. Westrum. *J. Chem. Thermodyn.* **10**, 949 (1978).
23. E. F. Westrum Jr., G. T. Furukawa, J. P. McCullough. *Experimental Thermodynamics, Vol. I, Calorimetry of Non-reacting Systems*, J. P. McCullough, D. W. Scott (Eds.), p. 133, Butterworths, London (1968).
24. Z. C. Tan, G. Y. Sun, Y. Sun, A. X. Yin, W. B. Wang, J. C. Ye, L. X. Zhou. *J. Therm. Anal.* **45**, 59 (1995).
25. V. I. Kosov, V. M. Malyshev, G. A. Milner, E. L. Sorkin. *Izmer. Tekh.* **11**, 56 (1985).
26. R. M. Varushchenko, A. I. Druzhinina, E. L. Sorkin. *J. Chem. Thermodyn.* **29**, 623 (1997).
27. L. Wang. Ph.D. thesis. Dalian Institute of Chemical Physics, Chinese Academy of Sciences, Dalian, China (2001).
28. L. Wang, Z. C. Tan, S. H. Meng, D. B. Liang, G. H. Li. *J. Nanoparticle Res.* **3**, 483 (2001).
29. L. D. Zhang, C. M. Mo. *Nanostructural Material Science*, p. 253, Liaoning Science and Technology Publishing, Shenyang, China (1994).
30. L. Wang, Z. C. Tan, S. H. Meng, A. Druzhinina, R. A. Varushchenko, G. H. Li. *J. Non-Cryst. Solids* **296**, 139 (2001).
31. R. W. Millar. *J. Am. Chem. Soc.* **50**, 2653 (1928).
32. A. Tschöpe, R. Birringer. *Acta Metall. Mater.* **41**, 2791 (1993).
33. C. H. Shimate. *J. Am. Chem. Soc.* **69**, 218 (1947).
34. K. K. Kelley. *Ind. Eng. Chem.* **36**, 377 (1954).
35. L. Wang, Z. C. Tan, S. H. Meng, D. B. Liang, B. P. Liu. *Thermochim. Acta* **386**, 23 (2002).
36. R. H. Busey, W. F. Giauque. *J. Am. Chem. Soc.* **74**, 3157 (1952).
37. D. L. Martin. *Rev. Sci. Instrum.* **58**, 639 (1987).
38. H. J. Fecht. *Mater. Res. Soc. Symp. Proc.* **206**, 587 (1991).